Major Project-II

THERMODYNAMICS ANALYSIS OF COMBINED POWER AND STEAM JET EJECTOR REFRIGERATION CYCLE USING SOLAR HEAT SOURCE

Submitted in partial fulfillment of the requirement

for the award of the degree of

Master of Technology

In

Thermal Engineering

Submitted By

ROHIT GOYAL

Roll No. 2K12/THR/18

Under the guidance of

DR. RAJESH KUMAR

Associate Professor

Mechanical Engineering Department

DEPARTMENT OF MECHANICAL, PRODUCTION & INDUSTRIAL AND AUTOMOBILE ENGINEERING

DELHI TECHNOLOGICAL UNIVERSITY, DELHI

2012-2014

DECLARATION

I hereby declare that the work, which is being presented in this dissertation, entitled **"Thermodynamics analysis of combined power and steam jet ejector refrigeration cycle using solar heat source"** towards the partial fulfillment of the requirements for the award of the degree of Master of Technology with specialization in Thermal Engineering, from Delhi Technological University Delhi, is an authentic record of my own work carried out under the supervision of **DR. RAJESH KUMAR** Associate Professor, Department of Mechanical Engineering, at Delhi Technological University, Delhi.

The matter embodied in this dissertation report has not been submitted by me for the award of any other degree.

Rohit Goyal
2K12/THR/18
Place: Delhi
Date:

This is to certify that the above statement made by the candidate is correct to the best of my knowledge.

DR. RAJESH KUMAR
Associate Professor
Department of Mechanical Engineering
Delhi Technological University
Delhi-110042

CERTIFICATE

It is certified that Rohit Goyal Roll no. 2K12/THR/18, student of M.Tech Thermal Engineering, Delhi Technological University, has submitted the dissertation titled "**Thermodynamics analysis of combined power and steam jet ejector refrigeration cycle using solar heat source**" under my guidance towards the partial fulfillment of the requirements for the award of the degree of Master of Technology.

He has developed a mathematical computational model for performing the energy and exergy analysis of the combined power and steam jet ejector refrigeration cycle system using EES software. His work is found to be satisfactory and his discipline impeccable during the course of the project. His enthusiasm, attitude towards the project is appreciated.

I wish him success in all his endeavors.

DR. RAJESH KUMAR
Associate Professor
Department of Mechanical Engineering
Delhi Technological University
Delhi-110042

ACKNOWLEDGEMENT

Generally, individuals set aims, but more often than not, their conquest are by the efforts of not just one but many determined people. This complete project could be accomplished because of contribution of a number of people. I take it as a privilege to appreciate and acknowledge the efforts of all those who have, directly or indirectly, helped me achieving my aim.

I take great pride in expressing my unfeigned appreciation and gratitude to my guide, DR. RAJESH KUMAR, Associate Professor, Department of Mechanical Engineering, for his invaluable inspiration, guidance and continuous encouragement throughout this project work.

Rohit Goyal

2K12/THR/18

TABLE OF CONTENTS

LIST OF FIGURES

LIST OF TABLES

LIST OF SYMBOLS/ABBREVIATIONS

A_h	aperture area of heliostat, m^2
$\dot{E}$	exergy rate, kJ/s
$\Delta\dot{E}$	exergy change, kJ/s
SJERC	steam jet ejector refrigeration cycle
$\dot{Q}$	energy rate, kJ/s
RC	Rankine cycle
T_S	apparent Sun temperature, K
T	absolute temperature, K
$\dot{W}$	turbine work output, kJ/s
h	enthalpy, kJ/kg
$\dot{m}$	mass flow rate of water in Rankine cycle, kg/s
q	Solar radiation received per unit area, W/m^2
s	entropy, kJ/kg/K

Greek symbols

μ	entrainment ratio
η	efficiency, %

Subscript

C	condenser
CR	central receiver
DNI	direct normal irradiation
E	evaporator
SJE	steam jet ejector
HRSG	heat recovery steam generator

P	pump
T	turbine
d	diffuser
ms	Molten salt
s	steam, isentropic
fv	flash vapor
pf	primary fluid
mf	mixed fluid
h	heliostat field
m	mixing chamber
n	nozzle
$n1$	inlet of nozzle
$n2$	outlet of nozzle

1, 2, 3…….a, b, c…..state points in Fig.

ABSTRACT

Thermodynamic analysis of combined power and steam jet ejector refrigeration cycle using solar heat source using molten salt as the heat transfer fluid is performed. This cycle is an integration of Rankine cycle and steam jet ejector refrigeration cycle which could produce electricity and refrigeration output simultaneously. Both exergy destruction and losses in each component and hence in the overall system are determined to identify the causes and locations of the thermodynamic imperfection. The effects of some influenced parameters like direct normal irradiation (DNI), turbine back pressure, evaporator temperature, condenser temperature have been observed on first and second law performance. It is found that maximum irreversibility occurs in central receiver as 32.4% and second largest irreversibility of 25% occurs in heliostat field. The second law efficiency of the solar driven combined power and steam jet ejector refrigeration cycle is 16% which is much lower than its first law efficiency of 31%. Analysis clearly shows that performance evaluation based on first law analysis is inadequate and hence more meaningful evaluation must include second law analysis.

CHAPTER 1: INTRODUCTION

1.1. OVERVIEW

Many researchers, during last few years, have been concentrated on the utilization of solar energy as it is inexhaustible, clean, and safe source of energy. However, it is diffused and cyclic in nature. It is, therefore, needed subsystem and components that can gather and concentrate it for conversion as efficiently as possible [1-2]. Recently, rapid development occurred worldwide in the basic technology and market strategy for the concentrating solar power (CSP) technologies that exploits the conversion of the solar energy to high temperature heat for power production [3-5].

India has a rich solar energy resource and the average intensity of solar radiation received in India is 200 MW/km^2. Using the free available solar energy in the existed thermal power plant for feed water heating and low pressure steam generation can reduce not only the global warming problems but also can save the high share of natural energy resource.

1.2. LITERATURE REVIEW

In order to make better use of the concentrating solar power for their potential in reducing fossil fuel consumption and alleviating environmental problems, the combined power and refrigeration cycles have been explored for improving overall energy conversion efficiency.

Goswami et al. [6] proposed a new combined power and cooling thermodynamic cycle. It is a combined cycle because it produces both power and cooling simultaneously with only one heat source, using ammonia-water mixture as the working fluid. The proposed cycle takes advantage of the low boiling temperature of ammonia vapour so that it can be expanded to a low temperature while it is still in a vapour state or a high quality two phase state. Results showed that cycle is best suited for solar thermal power using low cost concentrating collectors with prospective to reducing the cost of a solar thermal power plant also the same could be used as a bottoming cycle.

Oliveira et al. [7] presented a system of the cooling capacity 5kW and the electrical output of 1.5kW at the average boiler temperature of 95ºC using the ozone friendly refrigerant n-pentane. The system was based on the combination of an ejector cycle heat pump with a turbine/generator group and is powered by solar collectors supplemented by a gas burner,

for periods of low solar radiation. Results show that nearly competitive costs can be achieved for the system in areas with a large demand for power generation and cooling. Also to assess the impact of the combined system on the environment, an emissions analysis was carried out, comparing the CO_2 emissions from the solar/gas and shows that the potential of the combined system for saving emissions is high when compared to coal fired production and is as good as a combined cycle gas turbine providing electricity and with a natural gas burner for providing heating.

Zhang and Lior [8] studied an NH_3/H_2O system operates in parallel combined cycle mode with an NH_3/H_2O Rankine cycle and NH_3 refrigeration cycle interconnected by absorption separation and heat transfer process. The performance of the combined cycle was evaluated by both energy and exergy efficiencies with good guidance for system improvement. The influences of the key parameters like solution concentration, cooling water temperature and Rankine cycle turbine inlet parameters on the cycle performance, have been investigated. Results of the analysis showed the energy and exergy efficiencies of the cycle are 27.7% and 55.7%, respectively. They also compared the results with other optional systems for separate generation of power and refrigeration having the same power output and refrigeration capacity and showed that the cogeneration system has higher energy and exergy efficiencies. The NH_3/H_2O system for combined power and cooling production has the disadvantages of toxicity and flammability, needs rectification and its employment in absorption system requires expensive heat exchangers, high maintenance cost, and complexity in construction. On the other hand steam jet ejector refrigeration cycle has the advantages of simpler construction, lower capital as well as maintenance cost, higher reliability and silent operation.

Alexis et al. [9] proposed a combined system which is utilized to extract the stream form steam turbine for a combined conventional Rankine cycle to heat up the cooling fluid in the steam ejector refrigeration cycle. The results showed that the ejector refrigeration unit is more economical than absorption unit. The performance of the cogeneration system by variation of parameters like ratio of electrical power generated to heat input, evaporator temperature of the ejector cycle were studied by developing a computer program.

Khattab and Barakat [10] used a simulation program to analyse the performance of the solar steam-jet cooling system under different design and operating conditions like the

supersonic flow conditions in the convergent divergent nozzle and the preceding supersonic and subsonic diffusers and constructed a set of design charts for the solar steam-jet cooling cycle and for the selection of the ejector dimensions. Their results showed that single glazed, black-coated flat plate collectors may be used as the source of generator heating with better performance for selectively coated double glazed or evacuated flat plate collectors.

Alexis and Rogdak [11] described mathematical model for a steam ejector refrigeration cycle and the results are compared with experimental data. The Thermodynamic analysis of a steam ejector refrigeration system was presented in this paper. The model also studied the shocking phenomena with assumption that the mixing process of the two streams, motive and secondary stream, occurs at constant pressure and the conservation of fluid momentum within it. Results showed that this model is satisfying the experimental data.

Srisastra and Aphornratana [12] proposed and tested a workless boiler feeding system which feeds the liquid condensate to the boiler by means of gravity force and the boiler pressure so the steam jet refrigeration system becomes independent from electricity. Results show that workless boiler feeding system can be applied to a steam ejector refrigerator without any degradation in system performance compared with a system employing a conventional mechanical boiler feed pump. The use of this workless boiler feeding system would make a steam ejector refrigerator become a true heat powered refrigeration cycle.

Meyer et al. [13] has designed steam jet ejector refrigeration experimental system, which varies the boiler operating temperature from 85–140°C, evaporator liquid temperatures range from 5-10°C while the water-cooled condenser temperature ranges from 15–35°C. They concluded that the steam jet ejector is a practical viable system at boiler temperatures below 100°C. In this paper a case study is investigated by taking the experimental data of a solar powered steam jet ejector air conditioner and concluded that Solar powered steam ejector air conditioning systems are technical and economical viable when compared to conventional vapour compression air conditioners. Such a system can utilise any of the flat plate or evacuated tube solar thermal collectors depending on the type of solar energy available.

Ameri et al. [14] studied the performance of Micro-gas turbine cogeneration and tri-generation systems that includes a steam ejector refrigeration system and Heat recovery Steam Generator (HRSG). It produces 200 kW power and exhaust gases produces saturated steam in HRSG which is used in the steam ejector refrigeration system to produce cooling

and leads to the saving of fuel consumption up to 23%. In the second part of this paper, exergy analysis of the system has been performed and shown that combustion chamber, heat exchanger and HRSG were recognized as the largest sources of exergy losses respectively.

All the previous investigations indicates that the energy and exergy analyses of solar driven combined power and steam ejector refrigeration cycle, which uses heliostat field and central receiver as the concentrator-receiver system, has not date been reported in the literature. Thus, the objective of the current study is to construct a theoretical framework for the energy and exergy analyses of solar thermal driven combined power and steam ejector refrigeration cycle using molten salt as the heat transfer medium. The refrigerant, water is used in the ejector refrigeration cycle, has zero ozone depletion potential and global warming potential. Steam jet refrigeration which is capable to produce cooling above 0^0C with low grade heat input along with the availability of solar thermal receiver temperature in the range of 500^0C-600^0C provides a domain of research for solar thermal driven steam operated combined power and cooling cycle which is greatly expected to produce a significant power output and cooling for air-conditioning purpose.

The proposed cycle is the integration of Rankine cycle for the power generation and steam jet ejector cycle which provides cooling for suitable range of refrigeration and air conditioning. The influences of key parameters, which include the direct normal irradiation (DNI), turbine back pressure, evaporator temperature, condenser temperature on the proposed cycle performance, have been studied.

1.3. OUTLINE OF THE THESIS

The thesis is formulated as,

- In the second chapter, theory of solar thermal power plants is discussed, which includes the detailing about solar thermal power collecting technologies, heat transfer fluid and specification of power plant.
- In the third chapter of steam jet ejector refrigeration system, detailed theory, history of steam jet, and working principle of the same has been discussed.
- In the fourth chapter, titled as System Description and Thermodynamic Analysis describes the proposed cycle and thermodynamic equations used in energy analysis and exergy analysis is discussed.
- In the fifth chapter, the results obtained after performing the energy and exergy analysis on the system and an elaborate discussion on the results obtained are presented.
- In the sixth chapter, the essence of whole thesis is presented in the form of conclusion.

CHAPTER 2: SOLAR THERMAL POWER PLANT

The sun is the source of the vast majority of the energy we use on earth. Maximum energy we utilize has undergone various transformations before it is finally turns into desired form. There are many applications for the direct use of solar thermal energy like solar cooking, crop drying, water heating, and space heating as well as cooling. It is a well understood technology and widely used in various countries all over the world. More or less solar thermal technologies have been the way of life in one form or another for centuries and have a well-known industrial base in most developed countries.

2.1 TECHNIQUES FOR COLLECTING SOLAR RADIATIONS

In the solar thermal power plant, solar energy is used to generate electricity by generating steam. Sun rays are concentrated using reflector or absorber or directly on copper tubes filled with water and painted black outside. The water in the tubes then boils and become steam. This steam is used to drive steam turbine, which in turn causes the generator to produce electricity [15].

There are three main types of concentrating solar power collecting systems: parabolic-trough, dish/engine, and power tower.

Parabolic-trough systems concentrate the sun's energy through long rectangular, curved (U-shaped) mirrors. The mirrors are tilted toward the sun and focused the sunlight on a pipe which is placed at the centre of the trough. The focussed sunlight heats the oil flowing through the pipe. This hot oil is then used to boil water in a conventional steam generator to produce electricity.

A dish/engine system uses a mirrored dish (similar to a very large satellite dish). The dish shaped surface collects and concentrates the sun's heat onto a receiver that absorbs the heat and transfers it to fluid. The heat causes the fluid to expand against a piston or turbine to produce mechanical power. Same is used to run a generator or alternator to produce electricity.

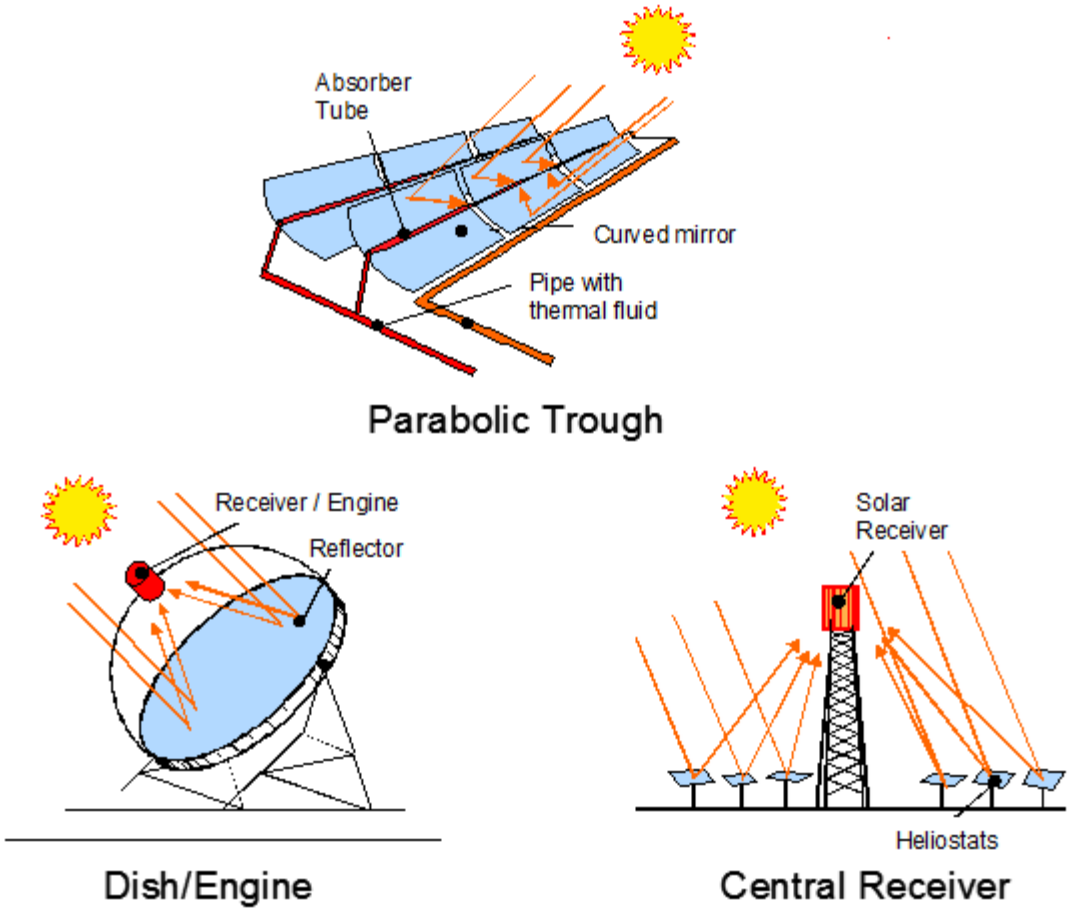

Fig. 2.1 Types of concentrating solar power systems

A power tower system used a large field of mirrors to concentrate sunlight onto the top of a tower, a receiver is placed there through which molten salt flows. This heated molten salt flowing through the receiver and HRSG to generate steam. Then, the steam is used to generate electricity through a conventional steam generator. Due to molten salt properties it can store heat efficiently for days before being converted into electricity. These advantages of the salt can produce electricity on cloudy days or even several hours after sunset. These kinds of plants are also called central Receiver Solar Power Plants.

A heliostat field consists of a large number of flat mirrors of 25 to 150 m^2 area which reflects the beam radiations onto a central receiver mounted on a tower. Each mirror is tracked on two axes. The absorber surface temperature may be 400 to 1000°C. The concentration ratio (total mirror area divided by receiver area) may be 1500. Steam, air or liquid metal may be used as working fluid.

Table 2.1 Range of temperature and concentration ratio for different types of solar thermal technologies [16]

Technology	**T (°C)**	**Concentration ratio**
Flat plate collector	30–100	1
Solar pond	70–90	1
Solar chimney	20–80	1
Evacuated tube collector	90–200	1
Non imaging trough	90–200	1.5-5
CLFR	260–400	8–80
Parabolic trough	260–400	8–80
Heliostat field with Central receiver	500–1200	600–1000
Dish concentrators	500–1200	800–8000

2.2 Heat Transfer Fluids:

In a concentrating solar power (CSP) installation thermal energy must be transported from the receiver by a primary heat transfer fluid (HTF). The properties of the primary HTF impose certain operational limits on the CSP plant and set a number of engineering challenges that are associated with that particular HTF. Two of the most prominent limitations are the maximum operational temperature and the melting point of the HTF. Low maximum operational temperature limits the thermal efficiency of the plant, and a high melting point may cause blockages in field or receiver pipes at night [17].

The impact of heat transfer properties and safety hazards can be found in the design considerations of a CSP plant, but mostly limited to receiver design, heat transfer flow rates in heat exchanger and plant working approaches, which are common engineering problems and do not causes the complete loss of plant efficiency.

The commonly used primary HTFs in CSP are:

1. **Thermal oil**
2. **Molten salt**
3. **Direct steam**

Table 2.2 Properties of heat transfer fluids [18]

HTF / Properties	Units	Sodium	NaK	Potassium	HitecXL	Hitec	Hitec solar salt	Dowtherm A
Melting point	*°C*	97.82	-12.6	63.2	120	142	240	15
Boiling point or maximum operating temperature	*°C*	881.4	785	756.5	500	538	593	400
Density	*kg/m^3*	820	749	715	1640	1762	1794	1056
Specific heat capacity	*kJ/kgK*	1.256	0.937	0.782	1.9	1.56	1.214	2.5
Viscosity	*Pa.s*	0.00015	0.00018	0.00017	0.0063	0.003	0.0022	0.0002
Thermal conductivity	*W/(m.K)*	119.3	26.2	30.7	N.A.	0.363	0.536	0.093

2.2.1. Thermal oil

Some parabolic trough collector (PTC) type solar plants use synthetic oil as a primary heat transfer fluid. There are various brands of synthetic oil heat transfer fluids. Artificial heat transfer oil like Dowtherm A is more stable at higher temperatures than that of mineral oil. They start to decompose at 400°C. At the maximum operating temperature the vapour pressure of Dowtherm A is 11 bars, which means that all the pipes, joints and receiver tubes must be designed to withstand high pressures. Thermal oil is highly flammable, specifically at high temperature. It is also hazardous to the environment if it should leak out of the system

2.2.2. Molten salt

Sensible heat storage in molten nitrate salt is one of the most prominent thermal storage mediums today. The high melting point of eutectic nitrate salts means that trace heating needs to be installed in the field piping to prevent the salt from freezing. Trace heating is where the HTF is heated to avoid freezing of fluid. Due to this reason it is preferable to use the salt as a primary HTF in a central receiver system where piping is contained within the tower and the power block.

Different molten salt mixtures are available but they generally have similar heat transfer characteristics. The most prominent high temperature salt is known as solar salt. It is a eutectic mixture of sodium nitrate (60 % by weight) and potassium nitrate (40 % by weight). Its melting point is 238°C, and working temperature range of between 260 to 567°C. It is non-toxic, non-flammable and has a low vapour pressure.

For lower temperature applications ternary eutectic products like Hitec and Hitec XL are used. These salt mixtures have melting points of about 100°C lower than that of solar salt, but their maximum operational temperature is between 500-538°C. These salts are more applicable for parabolic trough collector (PTC) applications. Table 2.2 shows the operative temperatures of some molten salts. Solar salt is better suited for high temperature applications.

2.2.3. Direct steam

Direct steam allows higher operational temperatures than possible with either molten salt or thermal oil. Theoretically it is possible to achieve superheated temperatures, but the high operating pressures are a controlling factor. Although it is possible to build a regular steam cycle running at supercritical pressures, which is a technical challenge to create receiver equipment able to control high pressures.

2.3 Integrated solar thermal power plants

In particular, in the field of large CSP plants, Integrated Solar Combined Cycle Systems (ISCCSs) are one of the most interesting options as they allow the achievement of a significant improvement in the conversion efficiency of solar energy and reduce the importance of energy storage systems. Moreover, ISCCS plants reduce solar energy production costs since the additional cost of the combined cycle steam section is lower than the overall cost of a dedicated steam power plant [19-20].

Most efficient method for converting solar thermal energy to electric energy is to withdraw feed water from the heat recovery steam generator (HRSG) downstream of economizer,

produce high pressure saturated steam using solar energy, and return the steam to the HRSG for superheating by the gas turbine exhaust.

This integrated plant was initially proposed by Luz Solar International in early 1990s, by incorporated a parabolic trough solar field with combined cycle power plant [21]. But because of economic reasons from 1990 to 2000 any new parabolic trough power plants have not been built. In 2000 due to the resolution of the Global Environment Facility, to provide grants for four ISCCS in India, Egypt, Morocco and Mexico, much attention in this kind of power stations increased all over again [22].

The ISCCS represents both economically and energetically a promising alternative for the conversion of solar energy while offering a guarantee of a minimum power supply independent of the level of solar radiation. However the performance is highly dependent on the intensity of the solar input and of the method of transferring solar energy into the combined cycle.

Several ways to optimize the performance of the ISCCS like different configurations, component design and system operation are proposed by [23-25], using a quasi-stationary approach based on pinch technology and showed that the minimum possible pinch point cannot be kept and the heat exergy losses are higher with solar energy input.

CHAPTER 3: EJECTOR REFRIGERATION SYSTEM

3.1 INTRODUCTION

The condensing type injector was invented by Henry Giffard in 1858. Primarily the injector was invented as a solution to problem of feeding liquid water to replenish the reservoir of steam engine boilers. But the possibility of using ejectors has been studied for a much different applications. In the past, ejectors have mostly been used in two different cycles for refrigeration purposes. In 1910, a new cycle introduced by Leblanc having a vapor jet ejector setup which allowed to produce a refrigeration effect by utilizing low-grade energy. Since then steam was widely available at that time, known steam jet refrigeration systems became popular in air-conditioning of large buildings and railroad cars. These days, same cycles are used to harness solar heat as well as other low-grade heat sources [26].

3.2 EJECTOR WORKING PRINCIPLE

A typical ejector consists of a nozzle, suction chamber, mixing section, and diffuser. The working principle of the ejector is based on converting internal energy and pressure related flow work contained in the motive fluid stream into kinetic energy. The nozzle is typically of a converging-diverging design. This allows the high-speed jet exiting the nozzle to become supersonic.

Fig. 3.1 shows the schematic view of a typical steam ejector. As the high pressure steam known as primary fluid (P), expands and accelerates through the primary nozzle (i), it fans out with supersonic speed to create a very low pressure region at the nozzle exit plane (ii) and subsequently in the mixing chamber. Secondary fluid (S), can be entrained into the mixing chamber. The primary fluid expanded wave was expected to flow and form a converging duct without mixing with the secondary fluid. At that cross-section across the duct, the speed of secondary fluid becomes sonic (iii) and chokes. Then the mixing process begins after the secondary flow chokes. This mixing causes the primary flow to be retarded whilst secondary flow is accelerated. By the end of the mixing chamber, the two streams are completely mixed and the static pressure was assumed to remain constant until it reaches the throat section (iv). Due to a high-pressure region downstream of the mixing chamber s throat, a normal shock of essential zero thickness is induced (v). This shock causes a major compression effect and a sudden drop in the flow from supersonic speed to subsonic speed. Auxiliary compression of the flow is attained (vi) as becomes stagnated through a subsonic

diffuser.

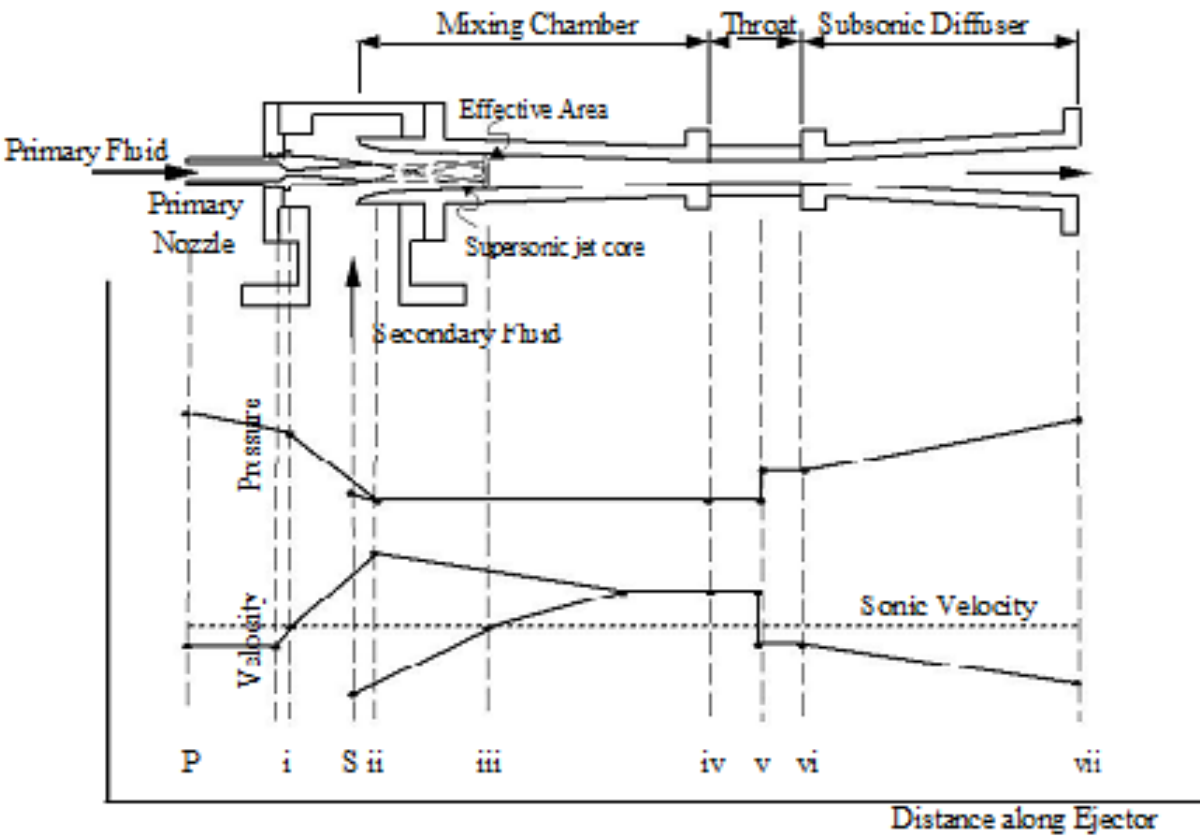

Fig. 3.1 Schematic view and the variation in stream pressure and velocity as functions of location along a steam ejector [27]

3.3 EJECTOR ANALYSIS

Ejector performance is dependent upon entrainment ratio which determines the magnitude of mass flow rate of secondary flash vapor to mass flow rate of primary motive steam coming out from the turbine. The basic principle of the model was introduced by Keenan et al. [29] based on gas dynamics and formulated by Huang et al. [30] and Ouzzanee et al. [31]. The formulation and assumption of entrainment ratio is based on mass, momentum and energy equations which is recently developed by Dai et al. [32] and may be reported as

$$\mu = \sqrt{\eta_n \eta_e \eta_d (h_{pf,n1} - h_{pf,n2,s}) / (h_{mf,d,s} - h_{mf,m})} - 1 \qquad (3.1)$$

The ejector mainly consists of three sections that is nozzle, mixing and diffuser section. In the nozzle section, the energy conservation equation for the adiabatic and steady primary flow is given as

$$\dot{m}_{pf} h_{pf,n2} + \frac{\dot{m}_{pf} u_{pf,n2}^2}{2} = \dot{m}_{pf} h_{pf,n1} + \frac{\dot{m}_{pf} u_{pf,n1}^2}{2} \tag{3.2}$$

The nozzle efficiency may be defined as

$$\eta_n = \frac{h_{pf,n1} - h_{pf,n2}}{h_{pf,n1} - h_{pf,n2,s}} \tag{3.3}$$

In the mixing section, the momentum conservation equation is given as

$$\dot{m}_{pf} u_{pf,n2} + \dot{m}_{sf} u_{sf,n2} = (\dot{m}_{pf} + \dot{m}_{sf}) u_{mf,m,s} \tag{3.4}$$

In the diffuser section, the energy equation is given as

$$\frac{1}{2}\left(u_{mf,m}^2 - u_{mf,d,s}^2\right) = h_{mf,d,s} - h_{mf,m} \tag{3.5}$$

The diffuser efficiency is given as

$$\eta_d = \frac{h_{mf,d,s} - h_{mf,m}}{h_{mf,d} - h_{mf,m}} \tag{3.6}$$

CHAPTER 4: CYCLE DESCRIPTION AND THERMODYAMIC ANALYSIS

4.1 DESCRIPTION OF THE PROPOSED CYCLE

The proposed system consists of Rankine cycle (RC), steam jet ejector refrigeration cycle (SJERC) with only solar heat source. Fig. 4.1 shows the simplified RC, SJERC, while Fig.4.2 depicts the corresponding T-s diagram. Solar energy falls on the heliostat field, and reflected on the aperture area of central receiver which is located at the top of the tower. The concentrated rays fall onto the receiver results in high temperature of the central receiver is used to heat the molten Salt (A mixture of 60%wt. $NaNO_3$+ 40%wt. KNO_3) Zavoico et al. [28].

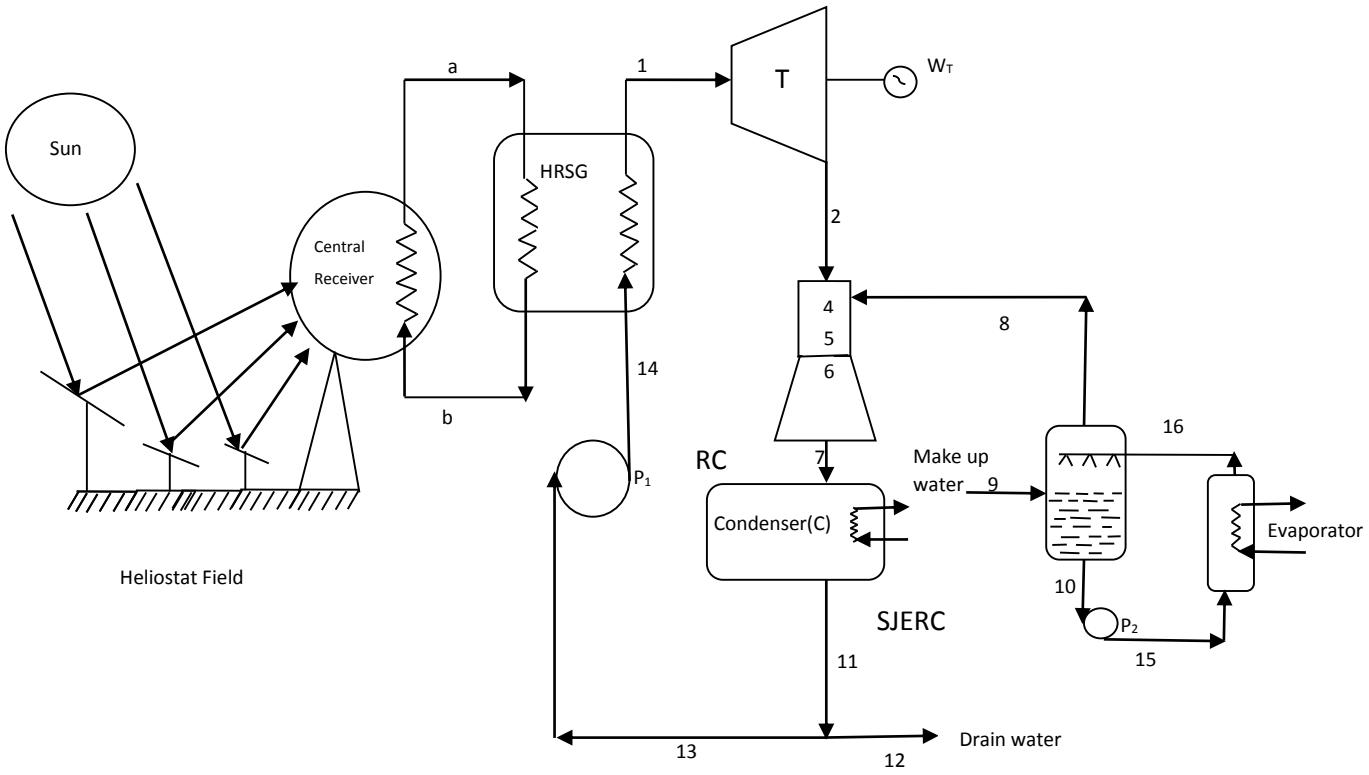

Fig. 4.1 Schematic diagram of solar driven combined power and steam jet refrigeration cycle

The Molten salt is flowing through the pipes which transfer the thermal energy from central receiver to the HRSG (a-b). Superheated steam (1) is expanded in a turbine to generate work (W_T).The turbine exhaust (2) passes through converging diverging supersonic nozzle of steam jet ejector (SJE). This very high velocity steam at the exit of the nozzle creates a very high vacuum at the inlet of the mixing chamber and extracts secondary flash vapors (8) into

the chamber from the flash camber of SJERC, which causes the cooling effect in the flash chamber. The primary motive steam (2) and secondary flash vapors (8) are mixed in the mixing chamber. After mixing the combined stream becomes supersonic and velocity of the combined stream is high enough to increase the pressure after declaration in the diffuser to the condenser pressure. The mixed stream (7) is cooled in condenser(C). The saturated liquid (11) is divided in two parts (12, 13), one part (12) is drained to the surroundings and second part (13) is pumped by pump (P_1) to the HRSG of RC cycle. The solar thermal energy (b) coming out from HRSG re-circulated to the central receiver. The make-up water is supplied through the inlet (9).

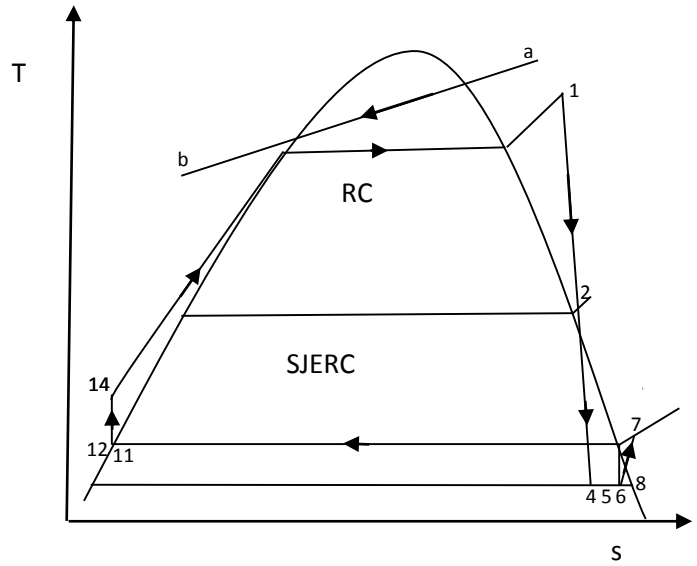

Fig. 4.2 T-s diagram of solar driven combined power and steam jet ejector refrigeration cycle

The following assumptions are made for the analysis of the proposed cycle:

- The components of the cycle are in steady state with constant solar radiation, and pressure drop in pipes and heat losses to the environment in the HRSG, turbine, ejector, condenser and evaporator are neglected.
- The condenser outlet state is saturated water.
- The evaporator outlet state is saturated vapor.
- Kinetic, potential and chemical exergies of the substances are neglected.
- Amount of power consumed by refrigerant pump is found to be negligible, hence it is assumed to be zero.

Note that, the properties of the heliostat, central receiver, nozzle, mixing chamber, and diffuser are reported in Table 5.1 and the required enthalpy values at various state points of the steam jet ejector cycle for refrigerant (water) are taken from REFPROP 6.01 [33]

4.2 **THERMODYNAMIC ANALYSIS**

A thermodynamic analysis considering both the first and the second laws of thermodynamics provides an opportunity to evaluate the theoretical performance of the proposed cycle. The model based on thermodynamic analysis able to predict the cycle performance, efficiency and emissions. Exergy analysis which is the combined application of both first and second laws of thermodynamics determines the system performance based on exergy which is defined as the maximum amount of work produced during the reversible transition of a stream of matter from its given thermodynamic state to the restricted dead state where the stream of matter will only be in thermal and mechanical equilibrium with the environment not in chemical equilibrium, hence the exergy obtained during this process will be the physical exergy.

Mathematically,

$$\dot{E} = \dot{m}[(h - h_0) - T_0(s - s_0)] \tag{4.1}$$

According to Bejan et al. [34], the entropy generation over a control volume is given by

$$\dot{S}_{gen} = \frac{dS}{dt} - \sum_{i=o}^{n} \frac{\dot{Q}_i}{T_i} - \sum_{in} \dot{m}s + \sum_{out} \dot{m}s \geq 0 \tag{4.2}$$

The exergy destruction and entropy generation are related as

$$\dot{E}_D = T_0 \, \dot{S}_{gen} \tag{4.3}$$

4.2.1 First law Efficiency (η_I)

It can be defined as the ratio of the desired output ($\dot{Q}_E, \dot{W}_T$) to the thermal energy of solar input ($\dot{Q}_{Solar}$). The first law efficiency of the combined power and steam jet ejector refrigeration cycle is then given by

$$\eta_I = \frac{\dot{Q}_E + \dot{W}_T}{\dot{Q}_{Solar}} \tag{4.4}$$

4.2.2 Second law Efficiency (η_{II})

Since exergy is more valuable than energy according to the second law of thermodynamics, it is useful to consider both output and input in terms of exergy. The amount of exergy supplied in the product to the amount of exergy associated with the fuel is more accurate measure of the thermodynamic performance of the system which is defined as the ratio of exergy contained in the product to the exergy associated with the fuel input and the second law efficiency of combined cycle may be reported as

$$\eta_{II} = \frac{\Delta \dot{E}_E + \dot{W}_T}{\dot{E}_{Solar}} \tag{4.5}$$

Where $\Delta \dot{E}_E$ the change in exergy at evaporator of ERC is, $\dot{W}_T$ is the work output of RC and $\dot{E}_{Solar}$ is the exergy associated with solar radiation falling on heliostat.

Equations have been applied to evaluate the energy and exergy balance and hence the equations for exergy destruction for each component of the proposed solar driven combined power and steam jet ejector refrigeration cycle are been provided.

4.3 ENERGY ANALYSIS

The first law of thermodynamics (energy analysis) is related to energy and work losses, while the second law of thermodynamics (exergy analysis) takes entropy into account via irreversibilities [34].

Applying steady flow energy to various components and neglecting change in Kinetic energy and change in Potential energy, we obtained the following expressions.

Energy balance equations:

For Heliostat: A part of thermal energy received by heliostat is delivered to the central receiver and rest is lost to the environment

$$\dot{Q}_{Solar} = A_h q \tag{4.6}$$

Where A_h and q are the aperture area and solar radiation per unit area

$$\dot{Q}_{Solar} = \dot{Q}_{CR} + \dot{Q}_{lost,heliostat} \tag{4.7}$$

So, $\eta_{I,heliostat} = \dfrac{\dot{Q}_{CR}}{\dot{Q}_{Solar}}$ (4.8)

For Central Receiver (CR): A part of thermal energy received by central receiver is absorbed by molten salt and rest is lost to the environment

$$\dot{Q}_{CR} = \dot{Q}_{ms} + \dot{Q}_{lost,CR} = \dot{m}_{ms}\left(h_a - h_b\right) + Q_{lost,CR} \quad (4.9)$$

And the energy efficiency of the central receiver is determined by Xu et al. [35].

$$\eta_{I,CR} = \frac{\dot{Q}_{CR,abs}}{\dot{Q}_{CR,abs} + \dot{Q}_{CR,lost}} = \frac{\dot{m}_{ms}\left(h_a - h_b\right)}{\dot{m}_{ms}\left(h_a - h_b\right) + \dot{Q}_{CR,lost}} \quad (4.10)$$

For HRSG:

$$\dot{m}_{ms}(h_a - h_b) = \dot{m}_s(h_1 - h_2) \quad (4.11)$$

For turbine:

$$\dot{W}_T = \dot{m}_s(h_1 - h_2) \quad (4.12)$$

For pump:

$$\dot{W}_P = \dot{m}_s(h_{14} - h_{13}) \quad (4.13)$$

For steam jet ejector:

$$\dot{m}_s h_2 + \dot{m}_{fv} h_8 = h_7(\dot{m}_s + \dot{m}_{fv}) \quad (4.14)$$

For condenser:

$$\dot{Q}_C = (\dot{m}_s + \dot{m}_{fv})(h_7 - h_{11}) \quad (4.15)$$

For Evaporator:

$$\dot{Q}_E = \dot{m}_{fv}(h_8 - h_9) \quad (4.16)$$

4.4 EXERGY ANALYSIS

The second law of thermodynamics infer the concept of exergy, a powerful tool for analysing both the quantity and quality of energy utilization. Exergy is defined as the maximum amount of work obtainable when the stream of matter is brought from its initial state to the dead state by the processes during which the stream may interact only with the environment. The exergy balance is similar to an energy balance but has the fundamental difference that, while the energy balance is a statement of a law of conservation of energy, the exergy may be looked upon as a statement of law of degradation of energy.

Exergy analysis is a powerful tool in the design, optimization, and performance evaluation of energy systems. An exergy balance applied to a process or a whole plant tell us how much of the usable work potential, or exergy supplied as the inlet to the system under consideration has been consumed (irretrievably lost) by the process. The exergy destruction or irreversibility provides a generally applicable quantitative measure of process inefficiency. Analysing a multi-component plant indicates the total plant irreversibility distribution among the plant components, pinpointing those contributing most to overall plant inefficiency.

Exergy analysis is useful for improving the efficiency of energy-resource use, since it quantifies the locations, types and magnitudes of losses [34].

Exergy balance for a control region undergoing a steady-state process is expressed as

$$\dot{X}_i + \dot{X}_j^Q = \dot{X}_e + \dot{W}_j + \dot{E}D_j$$

$$\dot{X}_i = \sum_{IN} \dot{m}\, x$$

$$\dot{X}_e = \sum_{OUT} \dot{m}\, x$$

$$\dot{X}_j^Q = \sum \left[\dot{Q}_j \frac{T - T_o}{T}\right]$$

Where $x = (h - T_o s) - (h_o - T_o s_o)$

Where the first term on left hand and right hand side represent physical exergy (neglecting kinetic, potential and chemical exergy component) of stream of matter entering and leaving the control region respectively. The second term on left hand side and right hand side is thermal exergy flow, which gives exergy transfer rate corresponding to the heat transfer rate

Q̇ when the temperature at the control surface where heat transfer is occurring is T and exergy associated with work transfer to and from the control region. ĖDrepresents rate of exergy destruction.

4.4.1. Exergy Destruction(ED)

Irreversibilities such as friction, mixing, chemical reactions and heat transfer through a finite temperature difference, unrestrained expansion, non-quasi-equilibrium compression or expansion always generate entropy, and anything that generates entropy always destroys exergy. Exergy destroyed is a positive quantity for any actual process and becomes zero for a reversible process. Exergy destroyed represents the lost work potential and is also called the irreversibility or lost work.

Exergy destruction equations: The basic equations of exergy destruction rate in the components of RC, SJERC are written as follows:

$$\dot{E}_{Solar} = \dot{Q}_{Solar}\left(1-\frac{T_0}{T_S}\right) \tag{4.18}$$

Where, T_s is the apparent sun temperature, taken as 4500 K.

$$\dot{E}_a = \dot{m}_{ms}[(h_a - h_0) - T_0(s_a - s_0)] \tag{4.19}$$

$$\dot{E}_b = \dot{m}_{ms}[(h_b - h_0) - T_0(s_b - s_0)] \tag{4.20}$$

$\dot{E}_b$ is the exergy associated with incoming molten salt from receiver while $\dot{E}_a$ is the exergy associated with outgoing molten salt to the receiver.

For Heliostat: A part of exergy received by heliostat is delivered to the central receiver and rest is lost to the environment (irreversibility),

$$\dot{E}_{Solar} = \dot{E}_{CR} + \dot{E}_{lost,heliostat} \tag{4.21}$$

And $$\eta_{II,heliostat} = \frac{\dot{E}_{CR}}{\dot{E}_{Solar}} \tag{4.22}$$

For Central Receiver (CR): A part of exergy received by central receiver is absorbed by molten salt and rest is lost to the environment (irreversibility):

$$\dot{E}_{CR} = \dot{E}_{ms} + \dot{E}_{lost,CR} = \dot{m}_{ms}\, c_{p,ms}\left[T_a - T_b - T_0 \ln\left(\frac{T_a}{T_b}\right)\right] + \dot{E}_{lost,CR} \tag{4.23}$$

And the second law efficiency of the central receiver is determined by Xu et al. [35].

$$\eta_{II,CR} = \frac{\dot{E}_{ms}}{\dot{E}_{CR}} = \frac{1 - \dfrac{T_0 \ln\left(\dfrac{T_a}{T_b}\right)}{T_a - T_b}}{1 - \left(\dfrac{T_0}{T_s}\right)} \tag{4.24}$$

For HRSG:

$$\dot{E}_{D,HRSG} = T_0[\dot{m}_{ms}(s_a - s_b) + \dot{m}_s(s_2 - s_1)] \tag{4.25}$$

For turbine:

$$\dot{E}_{D,T} = T_0[\dot{m}_s\,(s_2 - s_1)] \tag{4.26}$$

For steam jet ejector:

$$\dot{E}_{D,SJE} = T_0[(\dot{m}_s + \dot{m}_{fv})s_7 - \dot{m}_s s_2 - \dot{m}_{fv} s_8] \tag{4.27}$$

For condenser:

$$\dot{E}_{D,C} = T_0(\dot{m}_s + \dot{m}_{fv})(s_7 - s_{11}) \tag{4.28}$$

For Evaporator:

$$\Delta\dot{E}_{D,E} = \dot{m}_{fv}[(h_8 - h_9) - T_0(s_8 - s_9)] \tag{4.29}$$

CHAPTER 5: RESULTS AND DISCUSSION

A mathematical computational model is developed for performing the energy and exergy analysis of the system using EES software [36]

Table 5.1 The input data assumed for the calculation of results are:

Environment Temperature , ˚C	27
Environment pressure , MPa	0.10135
Turbine inlet pressure, MPa	8
Molten salt outlet temperature , ˚C	567-644
Molten salt inlet temperature , ˚C	290
Solar radiation received per unit area, W/m^2	800-975
Apparent Sun temperature, K	4500
Heliostat aperture area, m^2	10000
Turbine back pressure range, MPa	0.475
Turbine isentropic efficiency, %	85
Evaporator temperature range, ˚C	4-11 or [277K - 284K]
Condenser temperature range, ˚C	36-43
Pump isentropic efficiency, %	100
HRSG efficiency, %	100
HRSG effectiveness	0.9
Nozzle efficiency, %	90
Entrainment efficiency , %	65
Diffuser efficiency , %	80
Energy efficiency of heliostat field, %	75
Exergy efficiency of heliostat field , %	75
View factor of central receiver	0.8
Emissivity of central receiver	0.8
Reflectivity of central receiver	0.04

5.1. RESULTS

The thermodynamics analysis of solar driven combined power and steam jet refrigeration cycle has been done and the effect of influenced parameters has been studied. Following parameters have been chosen in the range of its operation; direct normal irradiation (800-975W/m^2), turbine back pressure (0.300-0.475 MPa), evaporator temperature (4-11˚C) and condenser temperature (36-43˚C).

An extensive exergy analysis has been performed and the results obtained are arranged in the tabular form. Also the comparison between various parameters calculated, has been represented in figures and tables.

The first law efficiency of the solar driven combined cycle is obtained by first law analysis of the cycle. However the exergy destruction in each component and the second law efficiency is investigated by the second law analysis of the cycle. Exergy destruction in each component of the cycle is made non dimensional by expressing it as the percentage of the solar exergy input. The thermodynamics properties of molten salt are taken from Zavoico et al. [28] and that of water are taken from REFPROP 6.01[33].

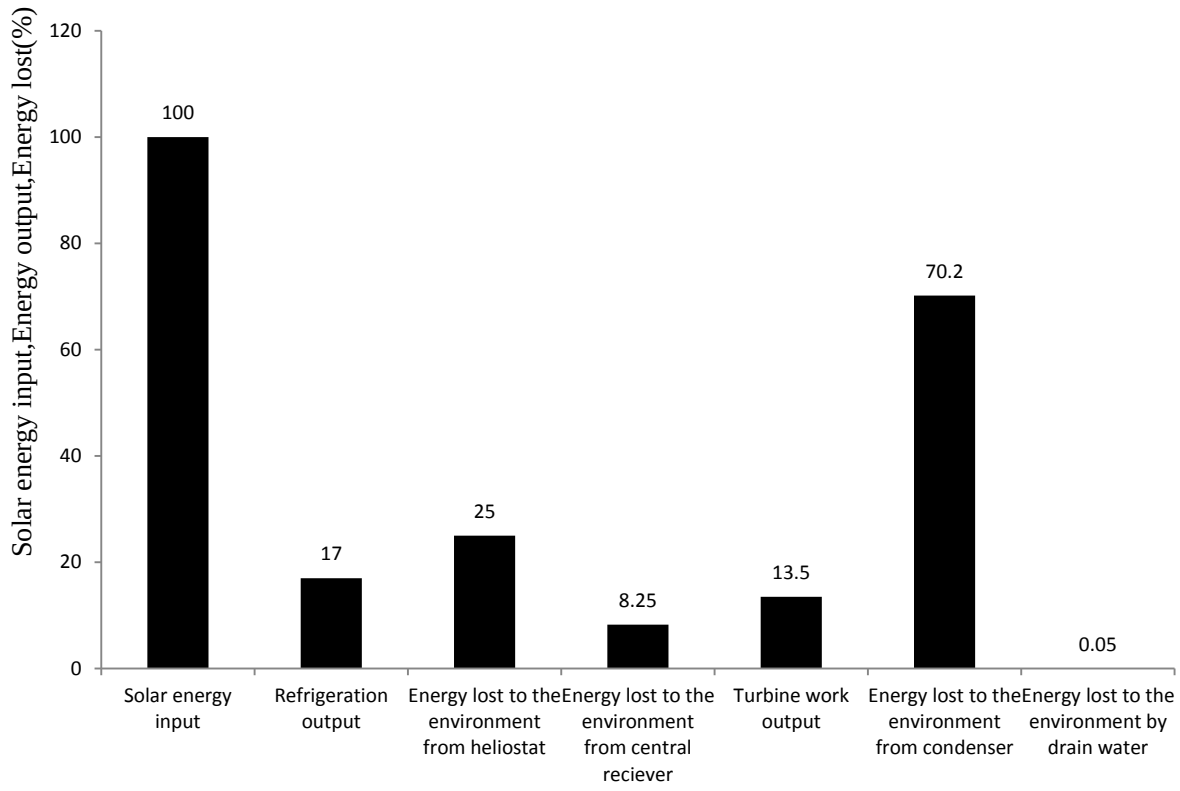

Fig. 5.1 Percentage(%) of solar energy input distribution in the solar driven combined power and steam jet ejector refrigeration system

First law analysis provides only the overall performance of the cycle while the second law analysis identifies and quantifies the sources of losses in the system. It helps to gain an insight into the system performance, therefore both energy and exergy distribution of proposed cycle is shown in Figures.

Fig. 5.1 indicates that out of 100 % solar thermal energy supplied to the system, around 30.5% is available as useful energy output(17% refrigeration output and 13.5% turbine work output),103.5%(Heliostat, central receiver, condenser, drain water energy loss) is lost to the environment from the system. Application of the second law analysis on the cycle found that around 16.03% of the solar thermal exergy input is available as exergy output (1.56% exergy

of refrigeration output and 14.47% turbine work output) and 83.97% of the input exergy is destructed in different components of the system, carried away by cooling water of condenser and drain water is shown as in Fig. 5.2. It is further observed that the central receiver and heliostat contributes the major exergy destruction while the condenser has the smallest.

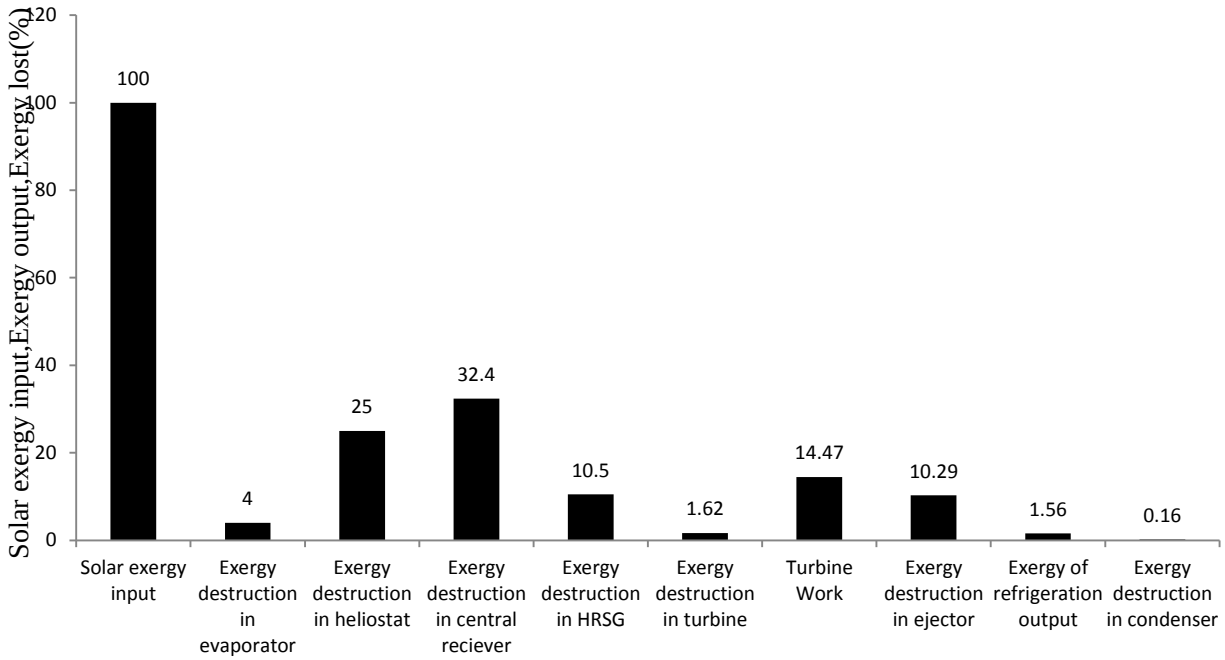

Fig. 5.2 Percentage(%) of solar exergy input distribution in the solar driven combined power and steam jet ejector refrigeration system

Fig. 5.3 shows the effect of the variation of direct normal irradiation (DNI) on first-law efficiency of the system, turbine work output and refrigeration output of combined power and steam jet ejector refrigeration cycle. The effect of variation of direct normal irradiation (DNI) on the energy and exergy efficiency of central receiver is discussed by Xu et al. [35]. First-law efficiency, refrigeration output and turbine work output increases with increase in direct normal irradiation. First law efficiency of the system varies from 30.7% to 31.4%, the refrigeration output and turbine work output are varying from 1403kW to 1730kW and 1054 kW to1333kW respectively. This is due to the fact that the increase in DNI increases the energy input into the system and also the first law efficiency of the central receiver. This increase causes the greater refrigeration output and turbine work output from the system.

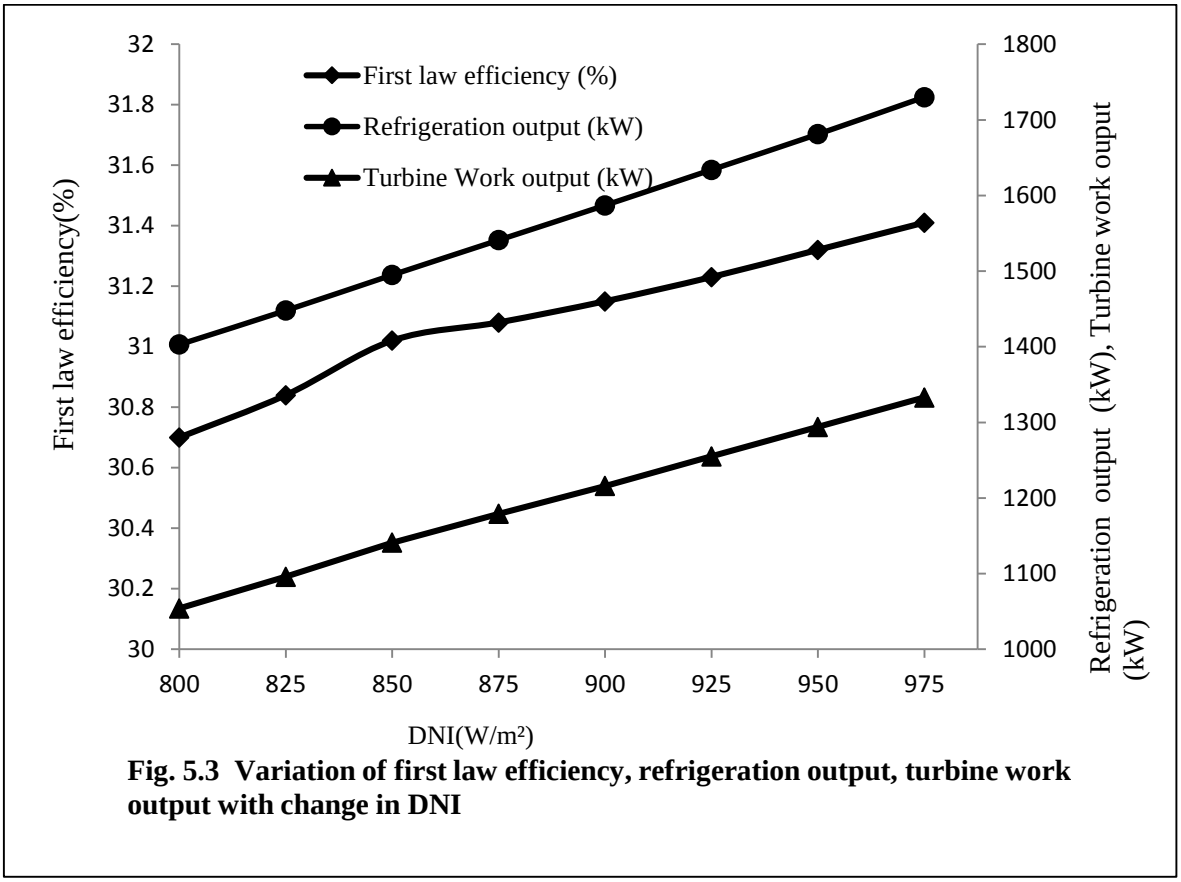

Fig. 5.3 Variation of first law efficiency, refrigeration output, turbine work output with change in DNI

Fig. 5.4 shows the variation of second law efficiency of the system, exergy of refrigeration output and turbine work output with the change in direct normal irradiation. It is found that second law efficiency of the system varies from 15.67% to 16.22%, while exergy of the refrigeration output and turbine work output lies between 111.7 kW to 142.6 kW and 1054 kW to 1333kW respectively. This is due to the fact that the increase in DNI increases the exergy input into the system and the marginally increase in second law efficiency of the central receiver. This increase causes the greater exergy of refrigeration output and turbine work output from the system.

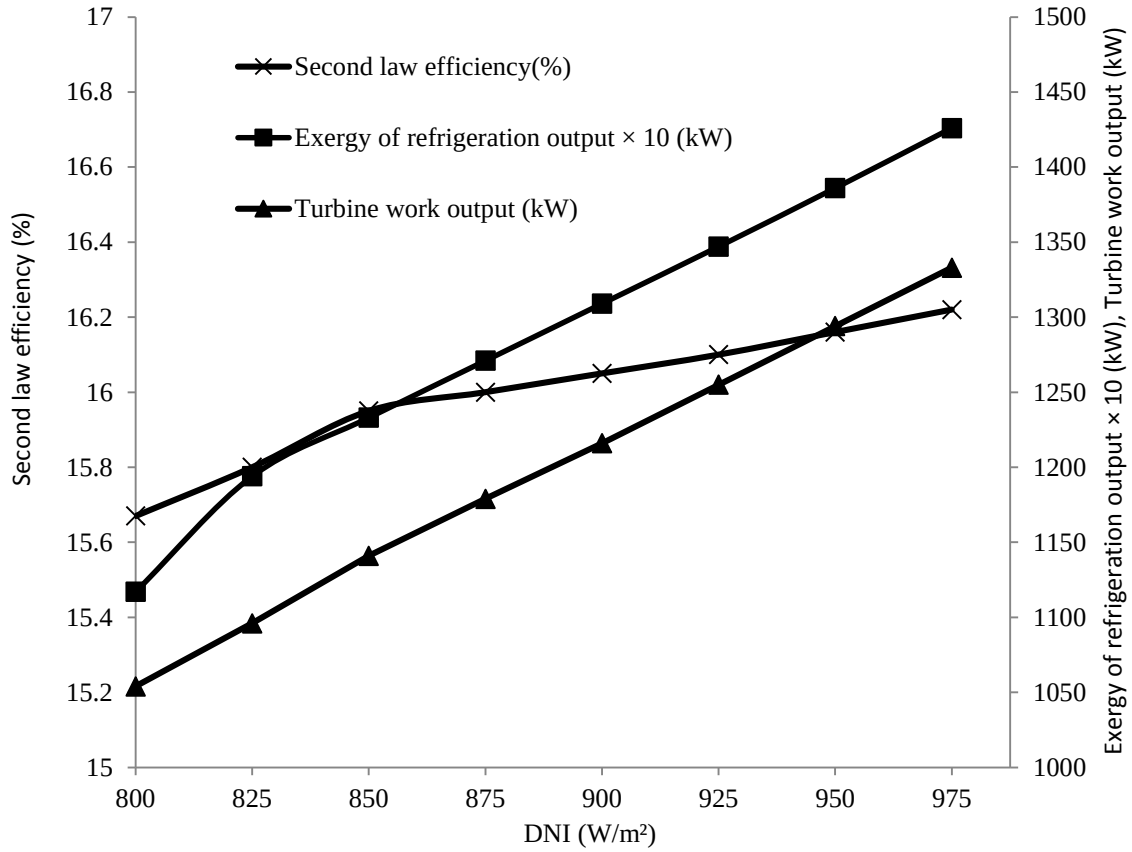

Fig. 5.4 Variation of second law efficiency, exergy of refrigeration output, turbine work output with change in DNI

Fig. 5.5 shows the effect of the variation in turbine back pressure on first-law efficiency of the system, refrigeration output and turbine work output of combined power and steam jet ejector refrigeration cycle for fixed direct normal irradiation (900W/m^2). First-law efficiency and refrigeration output increases while the turbine work output decreases with the increase in turbine back pressure. First law efficiency varies from 28.43% to 32.82% and refrigeration output and turbine work output are varying 1263 kW to 1787 kW and 1296 kW to 1167 kW respectively. This is due to the fact that as turbine back pressure increases the pressure ratio across the turbine decreases and hence the work output of the turbine decreases. But, as the turbine back pressure increase, there is an increase in the motive steam pressure which causes the suction of more water from evaporator and leads to the increase in the refrigeration output. But the increase in the refrigeration output is greater than the decreases in turbine work output which leads to the increase in first law efficiency of the system.

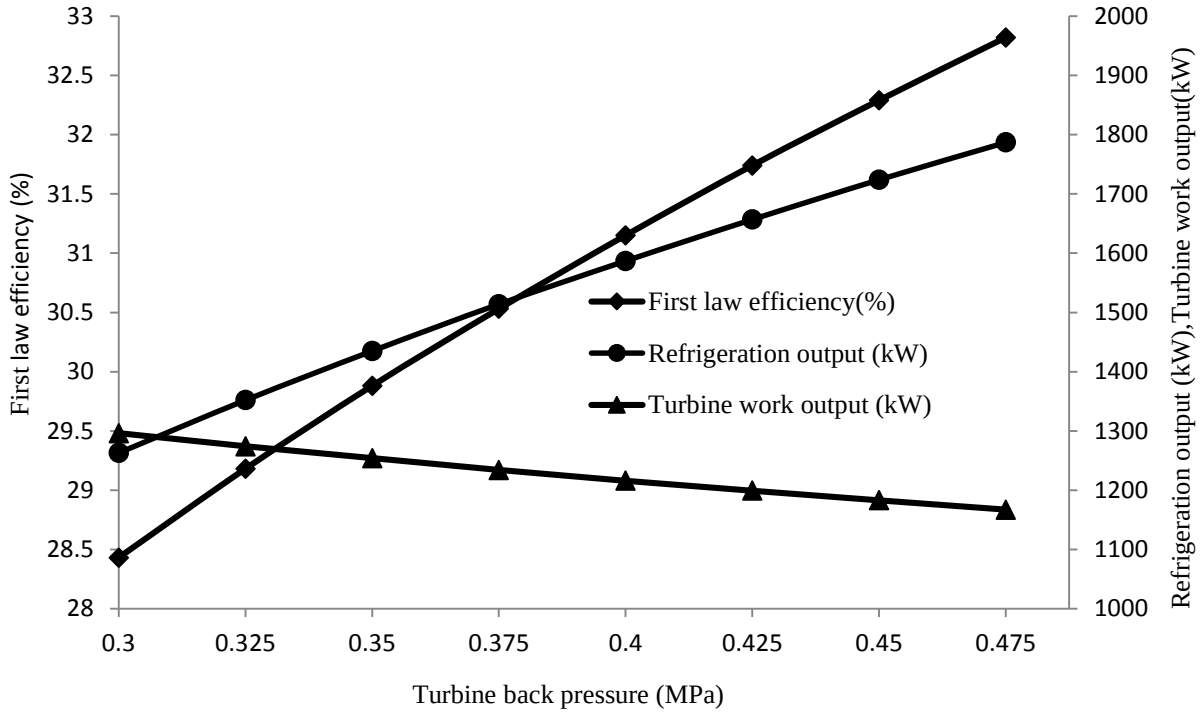

Fig. 5.5 Variation of first law efficiency, refrigeration output, turbine work output with change in turbine back pressure

The second law efficiency of the system varies with the change in turbine back pressure observed in Fig. 5.6. It is observed that second law efficiency of the system varies from 16.67% to 15.66%, while the exergy of refrigeration output and turbine work output lies between 104.2 kW to 147.3 kW and 1296 kW to 1167 kW respectively. This is due to the fact that as the turbine back pressure increases, there is high decrease in the turbine work output and small increase in the exergy of refrigeration output leads to the marginal decrease in the second law efficiency of the system.

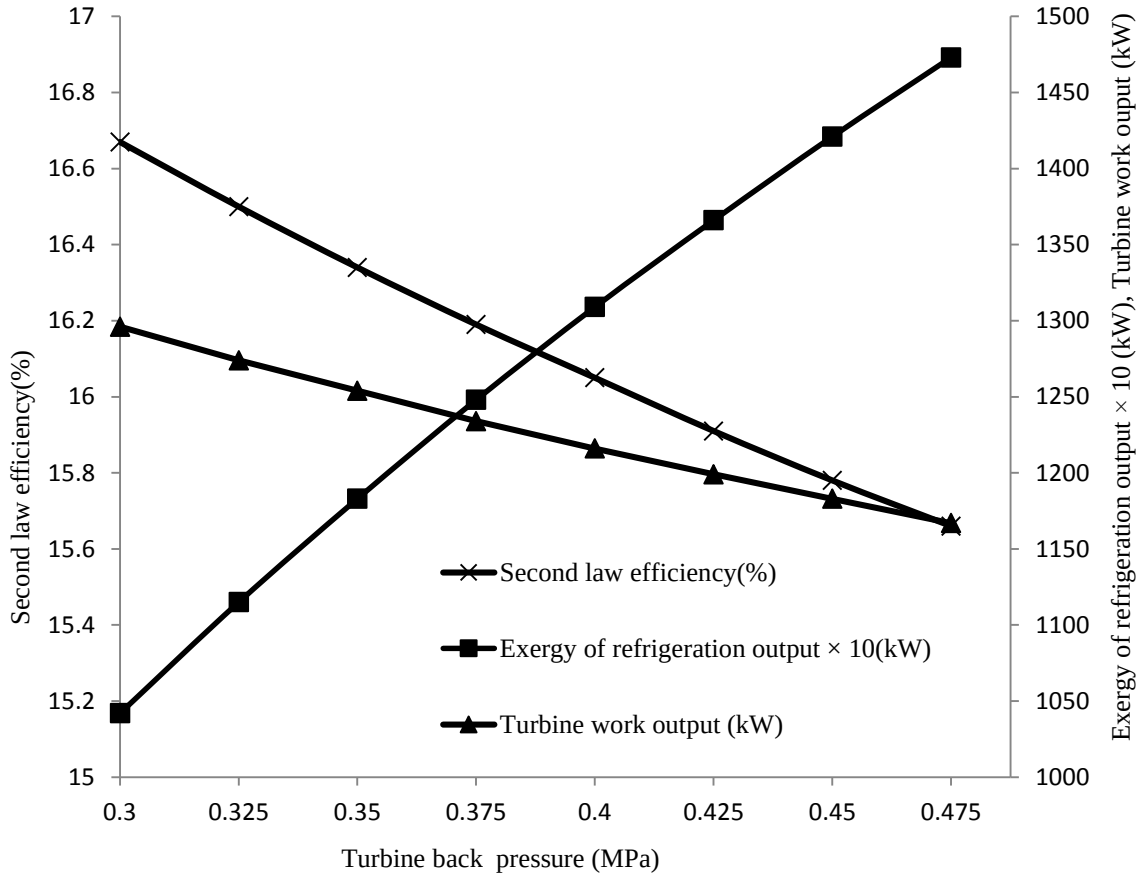

Fig. 5.6 Variation of second law efficiency, exergy of refrigeration output, turbine work output with change in turbine back pressure

Fig. 5.7 shows the effect of variation in evaporator temperature on the first-law efficiency of the system, turbine work output and refrigeration output of combined power and steam jet ejector refrigeration cycle. It is observed that the first law efficiency increases (31.15% to 43.66%) with the increase in ejector evaporator temperature because evaporator temperature increases the refrigeration output (1587 kW to 2713 kW) but the turbine work output (1216 kW) does not vary with the increasing evaporator temperature as the turbine inlet state and outlet state are not changed. With the increase in the evaporator temperature the mass flow rate of the secondary flash vapors entering into the steam jet ejector increases and hence, the refrigeration output and first law efficiency of the system increases.

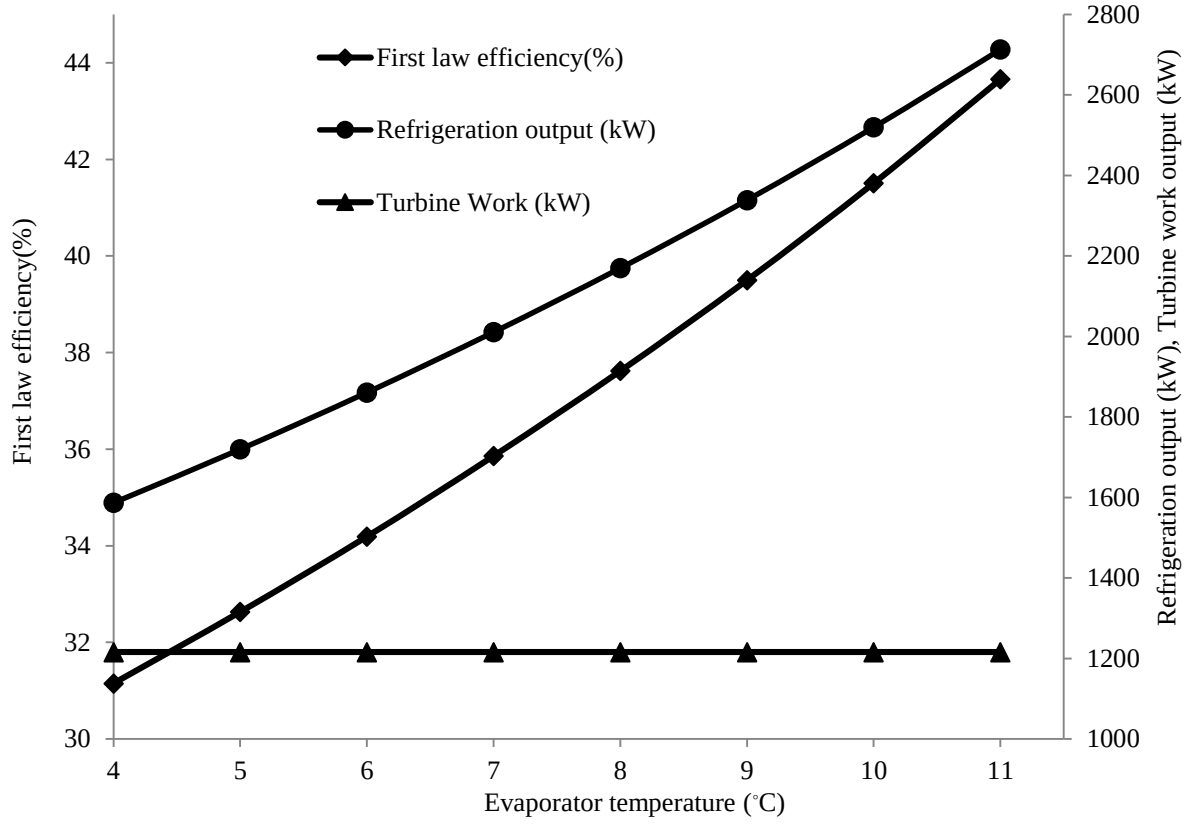

Fig. 5.7 Variation of first law efficiency, refrigeration output, turbine work output with change in evaporator temperature

Second law efficiency and the exergy of the refrigeration output of combined power and steam jet ejector refrigeration cycle increases with the increase in evaporator temperature while the turbine work output remains constant with the same as shown in Fig. 5.8. As the turbine work output remains constant with the increase in steam jet ejector evaporator temperature the change in second law efficiency of the system is only due to the marginal change in exergy refrigeration output which causes the marginal effect.

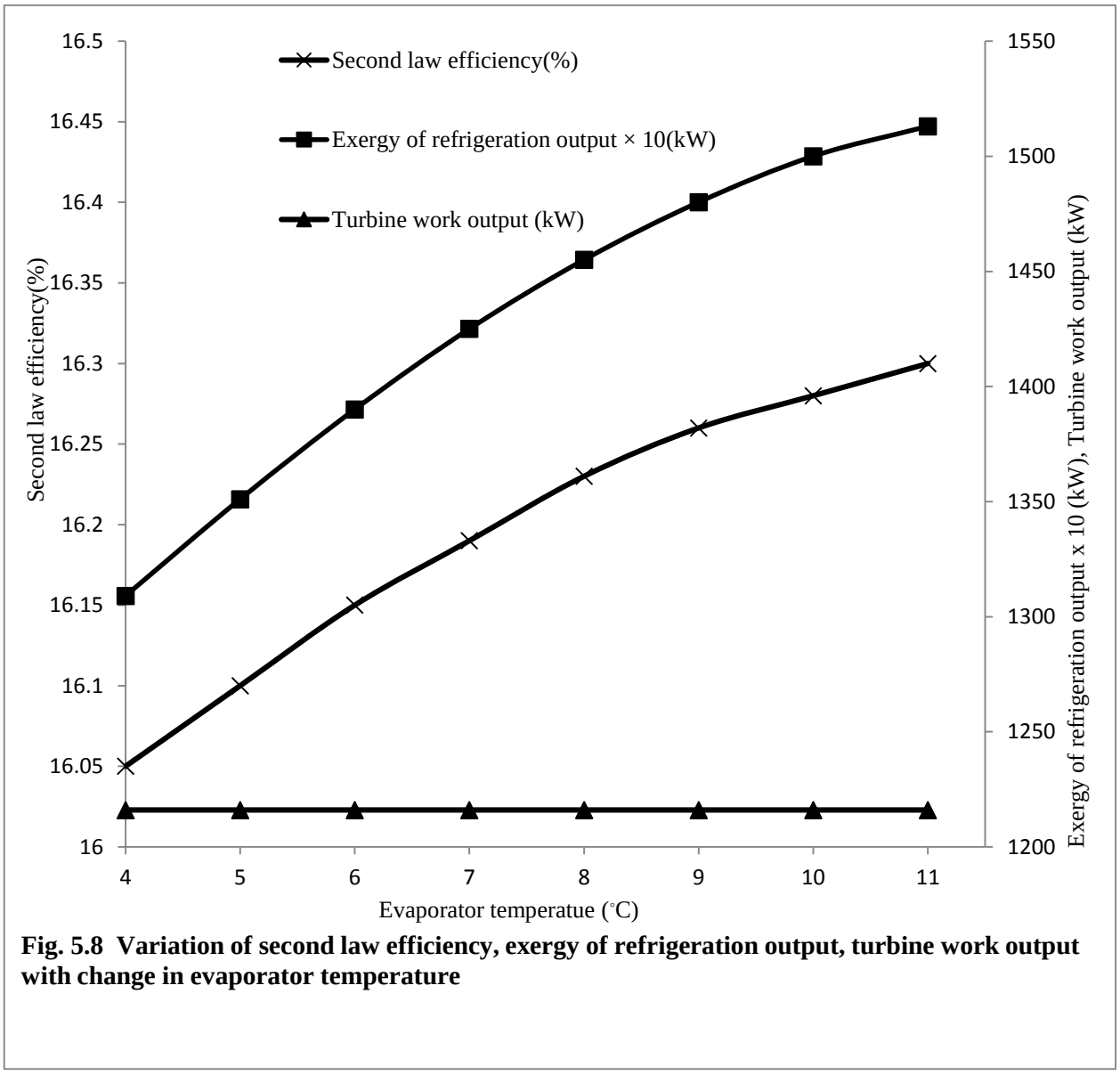

Fig. 5.8 Variation of second law efficiency, exergy of refrigeration output, turbine work output with change in evaporator temperature

Fig. 5.9 shows the effect of the change in condenser temperature on the first-law efficiency of the system, refrigeration output and turbine work output of combined power and steam jet ejector refrigeration cycle. It shows that the first-law efficiency of the system (38.53% to 26.60%) and refrigeration output (2257 kW to 1173kW) decreases significantly while the turbine work output remains same with increase in condenser temperature. This is because with the increase in condenser temperature the saturation pressure of the vapors coming out from the steam jet ejector is increased. This increased pressure at the steam jet ejector outlet results in decrease in the evaporation rate of the flash vapors from evaporator and consequently the refrigeration output and first law efficiency of the system is decreased.

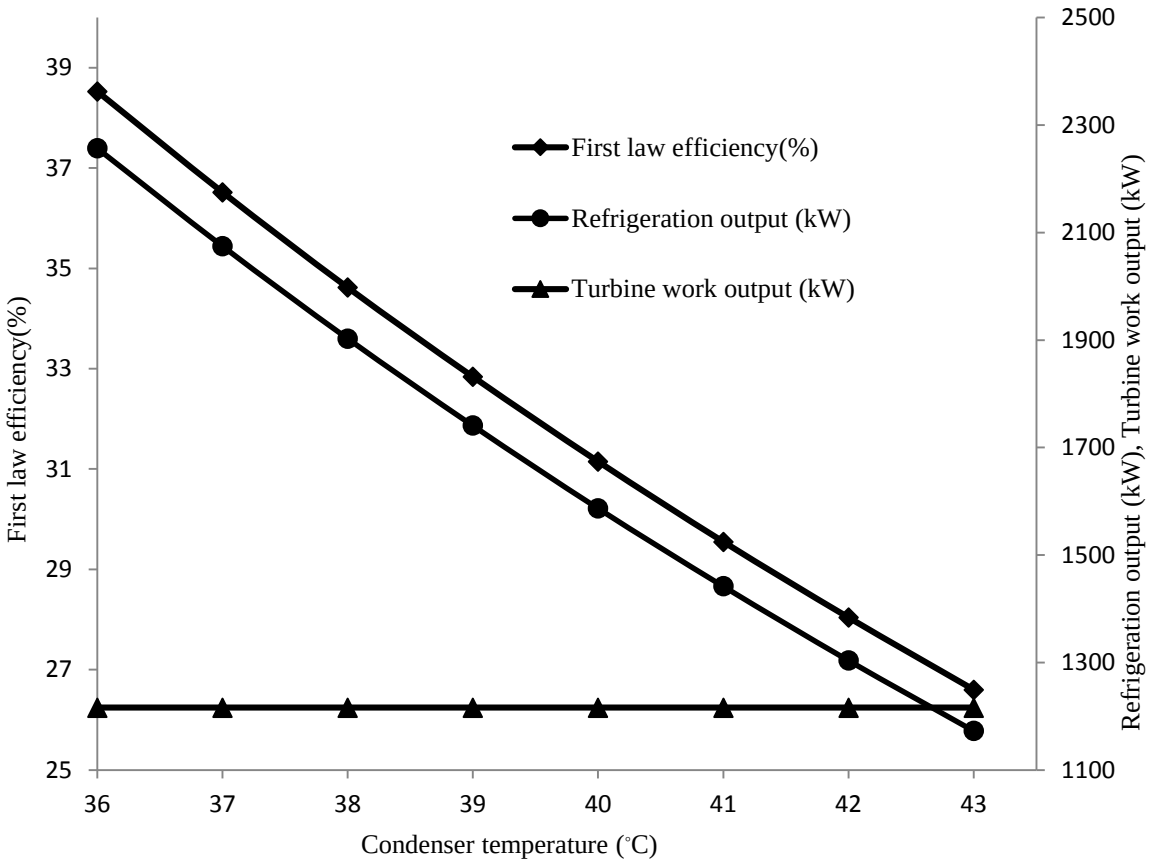

Fig. 5.9 Variation of first law efficiency, refrigeration output, turbine work output with change in condenser temperature

Almost a similar trend is observed for the second-law efficiency of the system, exergy of refrigeration output and turbine work output variation with the change in condenser temperature are observed in Fig. 5.10. It shows that second law efficiency of the system (16.63% to 15.70%) and the exergy of refrigeration output (186.1 kW to 96.7 kW) decreases but turbine work output remains constant.

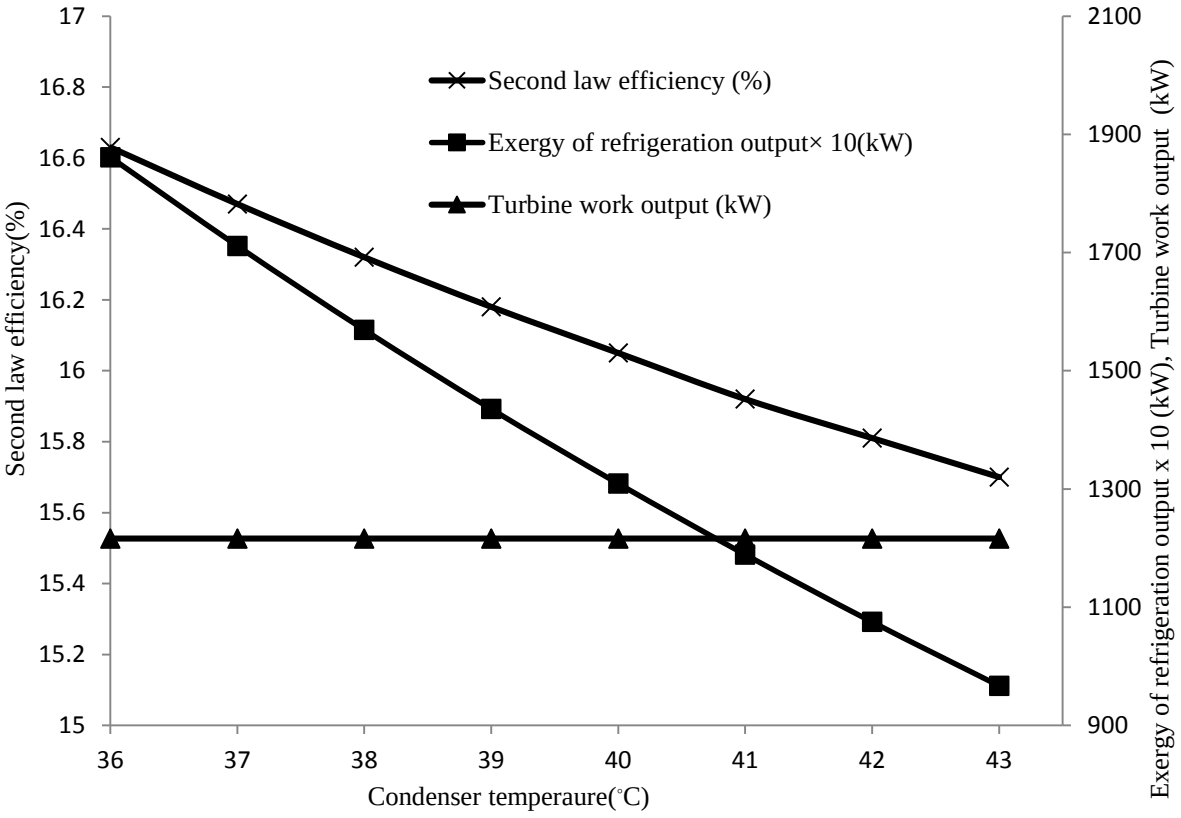

Fig. 5.10 Variation of second law efficiency, exergy of refrigeration output, turbine work output with change in condenser temperature

CHAPTER 6: CONCLUSION

A new solar driven combined power and steam jet ejector refrigeration cycle is proposed for the production electricity and cooling for air conditioning purpose. Energy and exergy methods are employed which enable us to develop a systematic approach that can be used to identify the sites of the real destructions/losses of valuable energy in thermal devices. The effect of several design parameters were observed on energy and exergy performance of the proposed cycle. The conclusions of the present analysis can be summarized as follows:

- Out of 100% energy (solar heat source) supplied to the system around 13.5% is produced as work output, 17% as refrigeration capacity and 103.5% is lost to the environment.
- Out of 100% exergy input, around 14.47% is produced as work output, 1.56% is available as exergy of refrigeration output and 83.97% is lost due to irreversibility in the components and via thermal lost to the ambient.
- For a given solar heat source, the exergy output of Rankine cycle is around 14.47% which is significantly higher than the exergy outputs of SJERC which is 1.56% .
- The largest contribution to cycle irreversibility comes from central receiver and heliostat field of 32.4% and 25%, respectively.
- The irreversibility of the order of 20.95% is observed in the HRSG, ejector and condenser of the SJERC.
- The exergy efficiency of around 16% for solar driven combined power and steam jet ejector refrigeration cycle is obtained which is much lower than its energy efficiency of 31%.

This comprehensive thermodynamic analysis provide a powerful and systematic tool for identifying the sources of real losses in solar driven combined power and steam jet ejector refrigeration cycle and guided for the effective exploitation of solar thermal energy using an integrated refrigeration system.

REFERENCES

[1] De Vos, Endoreversible thermodynamics of solar energy, Oxford University Press, USA, 1992.

[2] G. Harranz, A. Romero, V. de Castro, G. P. Rodriguez, Development of high speed steel sintered using concentrated solar energy, J. materials Processing Tech. 213 (2013) 2065–2073.

[3] S.M. Jeter, Maximum conversion efficiency for the utilization of direct solar radiation, Solar Energy 36(3) (1981) 231–236.

[4] M. Pingzhen, L. Wei, X Guoliang , Analytical and numerical Investigation of the solar chimney power plant systems , Int. J. Energy Res. 30(11)(2006) 861–873.

[5] S. M. Flueckiger , B. D. Iverson ,S. V. Garimella, J. E. Pacheco, System-level simulation of a solar power tower plant with thermo cline thermal energy storage, Appl. Energy 113(2014) 86–96.

[6] D.Y. Goswami, F. Xu, Analysis of a new thermodynamic cycle for combined power and cooling using low and mid temperature solar collectors, J.Solar Energy Eng.121(2) (1999) 91–-97.

[7] A. Oliveira, C. Afonso, J. Matos, S. Riffat, M. Nguyen, P. Doherty, A combined heat and power system for buildings driven by solar energy and gas, Appl. Therm. Eng. 22 (6) (2002) 587–93.

[8] N. Zhang, N. Lior, Development of a novel combined absorption cycle for power generation and refrigeration, J. Energy Resources Tech. 129(2007) 254–65.

[9] G. Alexis, Performance parameters for the design of a combined refrigeration and electrical power cogeneration system, Int.J. Refrig. 30(6) (2007) 1097–103.

[10] N. M. Khattab, M. H. Barakat, Modeling the design and performance characteristics of solar steam-jet cooling for comfort air conditioning, Solar Energy 73(4) (2002) 257–267.

[11] G.K. Alexis, E.D. Rogdakis, A verification study of steam-ejector refrigeration model, Appl. Therm. Eng. 23 (2003) 29–36.

[12] P. Srisastra, S. Aphornratana, A circulating system for a steam jet refrigeration system, Appl. Therm. Eng. 25 (2005) 2247–2257.

[13] A.J. Meyer, T.M. Harms 1, R.T. Dobson, Steam jet ejector cooling powered by waste or solar heat, Renew. Energy 34 (2009) 297–306.

[14] M. Ameri, A. Behbahaninia, A. A. Tanha, Thermodynamic analysis of a tri-generation system based on micro-gas turbine with a steam ejector refrigeration system, Energy35 (5) (2010)2203–2209.

[15] D. Yogi Goswami, Frank Kreith and Jan F.Kreider, Principles of Solar Engineering, 2nd edition. Taylor and Francis, Philadelphia, PA, (2000).

[16] John A. Duffie and William A Beckman,*Solar Engineering of Thermal Processes*, 2nd edition.Wiley, New York (1991).

[17] M. Medrano, A. Gil, I. Martorell, X. Potau, L.F. Cabeza, Renewable and Sustainable Energy Reviews, 14 (2010) 56-72.

[18] J.P. Kotzé, T.W. von Backström, P.J. Erens, A Combined Latent Thermal Energy Storage and Steam Generator Concept Using Metallic Phase Change Materials and

Metallic Heat Transfer Fluids for Concentrated Solar Power, Solar PACES 2011 – Granada

[19] M. Horn, H. Fuhring,J.Rheinlander, Economic analysis of Integrated Solar Combined Cycle power plants. A sample case: the economic feasibility of an ISCCS power plant in Egypt. Energy 29(2004) 935–945.

[20] R.Hosseini,M. Soltani, G. Valizadeh, Technical and economic assessment of the integrated solar combined cycle power plants in Iran.Renewable Energy 30(2005) 1541–1555.

[21] T. Achenbacj, Development of an edge module for open volumetric receiver for the use of the radiation at the receiver boundary region, Solar PACES 2011 – Granada

[22] TB Johansson,Renewable energy, sources for fuels and electricity. Washington, DC: Island Press; 1993, p. 234-5.

[23] Spencer Management Associates. Mexico feasibility study for an integrated solar combined cycle system (ISCCS). World Bank; 2000.

[24] Y.Allani, D.Favrat, M.von Spakovsky, CO2 mitigation through the use of hybrid solar combined cycles. Third Int. Conf. On Carbon Dioxide Removal Technologies (ICCDR-3), MIT, Cambridge, USA (1996).

[25] GE Cohen, DW Kearny,JKGregory. Final report on the operation and maintenance improvement program for concentrating solar power plants; (1999) SAND 99-1290.

[26] S.Elbel, P.Hrnjak,Experimental investigation of transcritical CO_2 ejector system performance, 22nd IIR International Congress ofRefrigeration, (2007) Paper ICR07-E1-72, Beijing, China.

[27] I.W. Eames, S. Aphornratana, H. Haider, A theoretical and experimental study of a small scale steam jet refrigerator, International Journal of Refrigeration 18 (6) (1995) 378–386.

[28] A.B. Zavoico, Solar power tower design basis document, Sandia National Laboratories, Report No. Sand2001-2100, 2001.

[29] H. Keenan, E.P. Neumann, F. Lustwerk, An Investigation of Ejector Design by Analysis and Experiment, Transactions of the ASME, J. Appl. Mech.72 (1950) 299–309.

[30] B. J. Huang, J. M. Chang, C. P. Wang, V. A. Petronko, A 1-D Analysis of Ejector Performance, Int.J. Refrig. 22(1999) 354–364.

[31] M. Ouzzane, Z. Aidoun, Model development and numerical procedure for detailed ejector analysis and design, Appl. Therm. Eng. 23(2003) 2337–2351.

[32] Y. Dia, J. Wang, L. Gao, Exergy analysis, parametric analysis and optimization for a novel combined power and ejector refrigeration cycle, Appl. Therm. Eng. 29(2009) 1983–1990.

[33] NIST Standard Reference Database 23, NIST Thermodynamic and transport properties of refrigerants and refrigerant mixtures REFPROP, Version 6.01,1998.

[34] A. Bejan, Fundamentals of exergy analysis, entropy generation minimization, and the generation of flow architecture, Int.J. Energy Res.26 (2002) 545–565.

[35] C. Xu, Z. Wang, X. Li, F. Sun, Energy and exergy analysis of solar power tower plants, Appl. Therm. Eng. 31(2011) 3904–3913.

[36] S.A. Klein,F.Alvarado,Engineering Equation Solver, F Chart software, Middleton, WI, Version 9.223, 2012.

APPENDIX

Table A.1 Variation of first law efficiency, refrigeration output, turbine work output with change in DNI

DNI (W/m²)	First law efficiency (%)	Refrigeration output (KW)	Turbine Work (KW)
800	30.7	1403	1054
825	30.84	1448	1096
850	31.02	1495	1141
875	31.08	1541	1179
900	31.15	1587	1216
925	31.23	1634	1255
950	31.32	1681	1294
975	31.41	1730	1333

Table A.2 Variation of second law efficiency, exergy of refrigeration output, turbine work output with change in DNI

DNI (W/m²)	Second law efficiency (%)	Exergy of refrigeration output × 10 (KW)	Turbine Work (KW)
800	15.67	1117	1054
825	15.8	1194	1096
850	15.95	1233	1141
875	16	1271	1179
900	16.05	1309	1216
925	16.1	1347	1255
950	16.16	1386	1294
975	16.22	1426	1333

Table A.3 Variation of first law efficiency, refrigeration output, turbine work output with change in turbine back pressure

Back Pressure (MPa)	First law efficiency (%)	Refrigration Effect (KW)	Turbine Work(KW)
0.3	28.43	1263	1296
0.325	29.18	1352	1274
0.35	29.88	1435	1254
0.375	30.53	1514	1234
0.4	31.15	1587	1216
0.425	31.74	1657	1199
0.45	32.29	1724	1183
0.475	32.82	1787	1167

Table A.4 Variation of second law efficiency, exergy of refrigeration output, turbine work output with change in turbine back pressure

Back Pressure(MPa)	**Second law efficiency (%)**	**Refrigation Exergy × 10(KW)**	**Turbine Work (KW)**
0.3	16.67	1042	1296
0.325	16.5	1115	1274
0.35	16.34	1183	1254
0.375	16.19	1248	1234
0.4	16.05	1309	1216
0.425	15.91	1366	1199
0.45	15.78	1421	1183
0.475	15.66	1473	1167

Table A.5 Variation of first law efficiency, refrigeration output, turbine work output with change in evaporator temperature

Te (°C)	**First law efficiency (%)**	**Refrigeration output (KW)**	**Turbine Work (KW)**
4	31.15	1587	1216
5	32.63	1720	1216
6	34.19	1861	1216
7	35.86	2011	1216
8	37.62	2170	1216
9	39.5	2339	1216
10	41.51	2520	1216
11	43.66	2713	1216

Table A.6Variation of second law efficiency, exergy of refrigeration output, turbine work output with change in evaporator temperature

T_e(°C)	Second law efficiency (%)	Exergy of refrigeration output × 10(KW)	Turbine Work(KW)
4	16.05	1309	1216
5	16.1	1351	1216
6	16.15	1390	1216
7	16.19	1425	1216
8	16.23	1455	1216
9	16.26	1480	1216
10	16.28	1500	1216
11	16.3	1513	1216

Table A.7 Variation of first law efficiency, refrigeration output, turbine work output with change in condenser temperature

Condenser Temp(°C)	First law efficiency (%)	Refrigeration output (KW)	Turbine Work (KW)
36	38.53	2257	1216
37	36.52	2075	1216
38	34.62	1903	1216
39	32.84	1741	1216
40	31.15	1587	1216
41	29.55	1442	1216
42	28.04	1304	1216
43	26.6	1173	1216

Table A.8 Variation of second law efficiency, exergy of refrigeration output, turbine work output with change in condenser temperature

Condenser Temp(°C)	Second law efficiency (%)	Exergy of refrigeration output× 10(KW)	Turbine Work(KW)
36	16.63	1861	1216
37	16.47	1711	1216
38	16.32	1569	1216
39	16.18	1435	1216
40	16.05	1309	1216
41	15.92	1189	1216
42	15.81	1075	1216
43	15.7	967	1216